

Grand paternal inheritance of an acquired metabolic trait induced by ancestral obesity is associated with sperm RNA

Jennifer E Cropley^{1,2*†}, Sally A Eaton^{1,2†}, Alastair Aiken¹, Paul E Young¹, Eleni Giannoulatou¹, Joshua WK Ho^{1,2}, Michael E Buckland³, Simon P Keam⁴, Gyorgy Hutvagner⁴, David T Humphreys¹, Katherine G Langley⁵, Darren C Henstridge⁵, David IK Martin⁶, Mark A Febbraio⁵, Catherine M Suter^{1,2*}

¹ Molecular, Structural and Computational Biology Division, Victor Chang Cardiac Research Institute, Darlinghurst, NSW, 2010, Australia.

² Faculty of Medicine, University of New South Wales, Kensington, NSW, 2052, Australia.

³ Brain and Mind Research Institute, University of Sydney, Sydney, NSW, 2006, Australia.

⁴ Faculty of Engineering and Information Technology, Centre of Health Technologies, University of Technology Sydney, Ultimo, NSW, 2007, Australia.

⁵ Cellular and Molecular Metabolism Laboratory, Baker IDI Diabetes and Heart Research Institute, Melbourne, VIC, 3004, Australia.

⁶ Children's Hospital Oakland Research Institute, Oakland, CA, 94609, USA.

* Correspondence to: c.suter@victorchang.edu.au; j.cropley@victorchang.edu.au

† These authors contributed equally to this work.

Abstract

Parental exposure to an environmental challenge can induce phenotypes in offspring independent of the inherited DNA sequence. Whether such acquired traits can be inherited – i.e., can manifest in a generation beyond that exposed to the precipitating insult as germ cells – is unclear. Here we report a latent metabolic phenotype induced by paternal obesity that is inherited into a second generation, without germ cell exposure. Sons of obese male mice exhibit defects in glucose and lipid metabolism that are only unmasked by post-weaning dietary challenge, yet they transmit these defects to their own progeny (F2) in the absence of the challenge. F1 sperm exhibit changes in the abundance of several small RNA species, including diet responsive tRNA-derived fragments. These data suggest that induced metabolic phenotypes may be propagated for multiple generations through the actions of noncoding RNA.

Introduction

Offspring phenotypes can be affected by parental health or parental environmental exposures, independent of variation in the inherited DNA sequence. Examples of such non-genetic transgenerational effects occur with a broad range of stressors, from dietary stress and toxin exposure to psychological stress or trauma (reviewed in ¹). In some instances, induced phenotypes can be observed across multiple generations, but whether such observations represent true inheritance of an acquired trait, or merely a residuum of the original exposure, is not clear. This distinction has adaptive significance for organisms living in a changing environment, given the potential for epigenetic states to respond to environment and selection^{2,3}.

In those cases in which induced phenotypes have been observed over more than one generation, determination of true inheritance is confounded by alternative scenarios. Persistence of an induced phenotype into grandoffspring of exposed mothers can generally be attributed to direct exposure of developing germ cells within the offspring. Such a scenario underpins several recent reports of programming by parental metabolism. For example, male mice exposed to a poor intrauterine environment can transmit metabolic defects to their own offspring⁴⁻⁶. An alternative scenario is serial programming of the induced phenotype over multiple generations: that is, when the phenotype induced in offspring mirrors the parental condition, and thus can in turn program defects in second generation offspring, *et cetera*. Serial programming resulting from a repeatedly compromised gestational environment may underlie most, if not all, examples of multigenerational maternal programming⁷.

It is currently unclear whether an induced metabolic phenotype can be transmitted into successive generations without the continued influence of the inducing stimulus; in other words, whether true, non-genetic transgenerational inheritance of a metabolic phenotype can

occur via gametes that were never exposed⁸. True inheritance of the effects of parental exposures is arguably best studied through the male lineage, where confounding effects of the intrauterine environment can be excluded. It is known that perturbed paternal metabolism can induce metabolic defects in first-generation offspring^{5,9-11}, but not whether the effects persist into second or subsequent generations. While epidemiological observations suggest this could be the case^{12,13}, the heritability of programming is difficult to ascertain in human cohort studies, where genetic heterogeneity, lifestyle factors, and the necessarily retrospective nature of longitudinal studies are major confounders.

We have addressed the question of inheritance directly using an isogenic rodent model of obesity and pre-diabetes. We used a dominant genetic mouse model of obesity in which the obesogenic allele can be segregated away from the offspring. In this model, paternal obesity induces a latent metabolic phenotype in first-generation sons that is unmasked by exposure to a high fat Western style diet. By breeding sons maintained on a healthy diet (exposed to paternal obesity but metabolically normal), we find that the latent phenotype induced by paternal obesity is inherited into a second, unexposed, generation. The inheritance is associated with changes to the small RNA profile of sperm in first-generation offspring, despite the sperm developing in a normal metabolic environment.

Results

Sons of obese sires carry a latent predisposition to hepatic insulin resistance

To model paternal obesity, we used C57BL/6 mice carrying the dominant *agouti viable yellow* (A^{vy}) mutation, which produces a phenotype of yellow fur, hyperphagia, and maturity-onset obesity¹⁴. Obese yellow A^{vy}/a males are hyperinsulinemic but not hyperglycaemic (Supplementary Fig. 1), modelling the majority of obese men of reproductive age who are insulin resistant but not frankly diabetic¹⁵. Obese A^{vy}/a heterozygote sires can be mated to congenic lean a/a dams to generate a/a offspring that are genetically identical to offspring from a/a matings. In this way, we generated two isogenic groups of F1 offspring differing only in the A^{vy} genotype, and the phenotypes, of their sires (see Supplementary Fig. 1 for breeding strategy and Supplementary Table 1 for breeding statistics). Offspring of each lineage were randomly assigned at weaning to either control diet (CD) or to a Western-style diet (WD) high in saturated fat and sugar (Supplementary Table 2).

When maintained on either CD or WD, weight trajectories of male a/a offspring of obese A^{vy}/a sires (PatObF1) were no different to offspring of lean sires (Fig. 1a). But while all animals gained weight on WD, PatObF1 animals gained more gonadal fat than controls (Fig. 1b), suggesting that paternal obesity confers an increased sensitivity to the adipogenic effects of a high-fat diet. Similarly, glucose tolerance was normal in all mice when maintained on CD (Fig. 1c), but after only three weeks on WD, PatObF1 males show a significantly impaired response in an intraperitoneal glucose tolerance test (Fig. 1d). The same degree of intolerance was observed whether the offspring were generated from an overnight timed mating or continuous co-housing of sire and dam (Fig. 1d); this indicates that the programmed defect was transmitted at the time of mating, rendering programming via social

effects of the obese sire on the dam or offspring improbable. PatObF1 males also had exacerbated hyperinsulinemia in response to WD (Fig. 1e), together with significantly elevated intrahepatic triacylglycerol (TAG), and the insulin resistance driver diacylglycerol (DAG) (Fig. 1f, g)¹⁶. These data indicate that paternal obesity programmed a latent predisposition to hepatic insulin resistance that was unmasked by challenge with a Western diet. We observed this programming only in males: for the duration of the experiment, female PatObF1 exhibited normal glucose homeostasis on both CD and WD (Supplementary Fig. 2).

The latent metabolic phenotype induced by paternal obesity is inherited from F1 sons into F2 grandsons

We then asked whether the defects programmed by paternal obesity could be inherited, that is, passed into a second, unexposed generation. Here the latency of the phenotype in F1 provides a material advantage in distinguishing inheritance from serial programming, since the germ cells and sperm of F1 mice on CD were not exposed to metabolic dysfunction. We found that the latent metabolic phenotype was inherited through the male line into F2: the PatObF2 males faithfully recapitulated the phenotype of their F1 sires. Again the weight trajectories of PatObF2 grandsons were no different from control (Fig. 2a), but PatObF2 had a greater gonadal fat mass on WD (Fig. 2b). With the WD challenge, PatObF2 grandsons exhibited the same pathognomonic signs of hepatic insulin resistance displayed by PatObF1 sons: marked glucose intolerance (Fig. 2d), hyperinsulinemia (Fig. 2e) and elevated hepatic TAG and DAG (Fig. 2f, g). The only contrast with the phenotype of F1 is that PatObF2 exhibited hyperinsulinemia and a mild glucose handling impairment even on CD (Fig. 2 c, e), suggesting that the phenotype inherited to F2 is slightly more overt than in F1. Taken together, these data indicate that the latent predisposition to metabolic defects induced by paternal obesity is inherited into a second, unexposed, generation. The germ cells that gave

rise to the F2 generation developed while the F1 mice were gestating in a normal intrauterine environment, and matured inside an F1 individual that was not obese and had no overt metabolic disturbance, arguing against serial programming as the mechanism of transmission. Thus we have observed true, non-genetic transgenerational inheritance of an acquired metabolic phenotype induced by ancestral obesity.

Inheritance of the latent metabolic phenotype into F2 is associated with changes in F1 sperm RNA content

The characteristics of the inheritance we observe implicate an epigenetic inheritance system. Small noncoding RNAs direct epigenetic states in the germline^{17,18} and have been implicated in invertebrate models of epigenetic inheritance¹⁹⁻²². Recently two separate studies have shown that the small RNA content of murine sperm is sensitive to dietary perturbations: both a low-protein diet and a high-fat diet are linked to changes in the abundance of specific small RNA species in exposed sperm^{11,23}. We asked whether small RNA perturbations may also underlie the *inheritance* of the induced metabolic phenotype we observe. To do this we examined the small RNA content of sperm from F1 offspring of obese sires fed the control diet: these males are able to transmit the latent phenotype, but do not exhibit it. We compared the sperm small RNA profiles with those from control-fed control males.

The distribution of small RNA lengths and biotypes between the two groups was very similar (Fig. 3a,b), but within two biotypes – miRNA and tRNA-derived fragments (tRFs) – there were major differences in abundance of some species. Using stringent thresholds (only considering miRNA with counts >200 per million, and adjusted *p*-value of < 0.05) we found 24 miRNAs with altered expression in PatObF1 (Figure 3c, Table 1). One sperm miRNA, miR-10, exhibited dramatic changes, increasing 2.5-fold to constitute ~25% of all sperm miRNA in PatObF1 (Fig. 3). Both miR-10 isotypes, miR-10a and miR-10b (encoded by

different genes) were significantly elevated. Differing only by one nucleotide which is outside of the seed sequence, these two miRs target the same set of mRNAs (Supplementary Table 3); these targets are heavily and significantly enriched for functions related to the regulation of transcription (Fig 3e).

Around a quarter of all sperm small RNAs were tRFs of two predominant species, tRF5-GluCTC and tRF5-GlyGCC: collectively, sequences of these two isotypes contributed ~90% of all sperm tRFs. The relative ratios of these tRFs were inverted in PatObF1 sperm relative to control sperm, with an ~30% reduction in tRF5-GluCTC and a corresponding increase in tRF5-GlyGCC (Fig. 3f). Another two tRFs, ValCAC and HisGTG were also significantly elevated in PatObF1 sperm, although these tRFs were much less abundant, constituting less than 5% of all sperm tRFs. Both tRF5-GluCTC and -GlyGCC display precise cleavage at the 5' side of the anticodon loop of the mature tRNA to generate fragments of predominantly 30 and 31 nucleotides, respectively (Fig. 3g). GluCTC and GlyGCC are the same tRFs that were reported as perturbed in sperm by exposure to an altered diet^{11,23}.

Mature sperm are transcriptionally and translationally inert, so any function of the sperm-borne tRFs and miRNAs is likely to manifest post-fertilisation. Recently reported diet-responsive tRFs induce transcriptional changes in the early embryo; whether this is a direct or indirect transcriptional effect is unclear. Available evidence indicates that tRFs reside almost exclusively in the cytoplasm²⁴ where they can associate with polyribosomes and affect translation²⁵⁻²⁷. The majority of miRNAs are also found in the cytoplasm and functionally associate with Ago2. Ago2 is highly expressed in the oocyte and early embryo and is required for the maternal-to-zygotic transition (MZT)²⁸. We asked whether the two sperm tRFs can also associate with Ago2, and found that tRF5-GluCTC, and to a lesser extent tRF5-GlyGCC, was enriched in an Ago2 pulldown (Fig. 3h). This indicates that at least tRF5-GluCTC binds

Ago2, signifying its potential to act in a miRNA-like manner in the zygote. Using a miRNA ‘seed’ sequence-based algorithm we identified potential tRF5-GluCTC targets: the individual predicted targets of tRF5-GluCTC shared very little overlap with those of miR-10, yet remarkably resided in strikingly similar transcriptional regulation ontologies (Fig. 3i,j, Supplementary Table 3). Using publicly available datasets of murine early embryonic transcription²⁹ we found that 114/220 miR-10 targets and 77/191 tRF-5-GluCTC targets are expressed in the oocyte; approximately half of these targets are reduced by at least two-fold at the 4-cell stage relative to the oocyte, consistent with a repressive post-transcriptional function of miR-10 and tRF-5-GluCTC.

Discussion

We have identified an acquired metabolic phenotype induced by paternal obesity that persists for two generations, independent of the inherited genotype, the gestating environment, and continued exposure to the inducing stimulus. The characteristics of our model – in particular the latency of the induced phenotype – strongly suggest that the transmission we observe represents true inheritance of an acquired phenotype. While there has been one previous report of a paternally-induced and inherited behavioural phenotype in mice³⁰, to our knowledge, this is the first clear demonstration of the inheritance of a paternally-induced metabolic phenotype in vertebrates. Our findings have immediate relevance to the evolution of human disease and suggest a mechanism by which the memory of ancestral exposures may be maintained through multiple generations.

In our model, obese founder males had a syndrome of obesity and hyperinsulinemia, but the F1 males that gave rise to the F2 generation did not. When maintained on a regular chow diet, F1 males were effectively indistinguishable from isogenic controls in terms of weight, glucose metabolism, insulin levels, and hepatic lipids; this argues strongly against the serial transmission of the metabolic defects from F1 to F2 and implies epigenetic inheritance. The possibility that the latent phenotype was transmitted by behavioural factors is also unlikely: dams partnered with obese sires were no heavier than dams of control sires, indicating that they did not acquire the hyperphagia of their partners, and the programmed phenotype was just as robust when the influence of the sire was restricted to an overnight timed-mating. The most parsimonious explanation for the transmission of the latent metabolic phenotype is transgenerational epigenetic inheritance: some mark or memory of paternal obesity passaged via the male germline, implicating sperm in the transmission.

We found alterations to multiple prominent small RNA species in the sperm of mice born of obese fathers. The idea that sperm RNA is involved in transgenerational epigenetic inheritance is well established in invertebrate systems. In the fly, small RNAs influence the transgenerational inheritance of maternal immunity to paternally-introduced transposons²². In the nematode *C. elegans*, small noncoding RNAs are implicated in multiple models of transgenerational inheritance^{19,20,31} including a metabolic starvation-induced response²¹. There is more limited, and somewhat controversial, evidence for small RNA involvement in inheritance of vertebrate phenotypes: injection of sperm RNA into fertilised oocytes has been reported to recapitulate several induced phenotypes, including white tail tipping³², cardiac hypertrophy³³ and fear conditioning³⁴.

Molecular changes to mouse sperm (including alterations to DNA methylation, miRNAs, and tRFs), have been described in response to environmental factors, including dietary perturbations^{4,6,10,11,23,34}, but in these studies sperm were directly exposed to the initiating stimulus, either as mature gametes or as developing germ cells. In this study we did not examine the directly exposed sperm (i.e. that from the obese founder males), because identification of any agent of inheritance may have been confounded by changes induced by direct exposure of the sperm to the syndrome of obesity and pre-diabetes. It is remarkable that we find alterations to the same tRF species as have been recently reported to be male diet-sensitive^{11,23}. The sperm from F1 males in our study were not exposed to obesity or altered diet, or indeed to any apparent insult at all, but they still transmitted the induced phenotype to the F2 generation. Together these data provide compelling evidence implicating tRFs and other small RNAs in the inheritance of acquired metabolic traits in vertebrates.

Given that mature sperm are transcriptionally and translationally inert, it is likely that sperm small RNAs function post-fertilisation. Recent work in *C. elegans* found that around half of

all small noncoding RNAs in the one-cell embryo are paternally derived³⁵. This raises the possibility that sperm-borne small RNAs play a role in very early development prior to, or during, the maternal-to-zygotic transition³⁶. Both of the recent studies that identified diet-regulated sperm tRFs found changes in early embryonic transcriptional invoked a direct transcriptional interference mechanism for sperm-borne tRFs^{11,25}. However, available evidence indicates that tRFs reside almost exclusively in the cytoplasm²⁴ where they can associate with polyribosomes and affect translation²⁵⁻²⁷. Our data suggest a post-transcriptional regulatory function that indirectly affects transcription. The targets of the two small RNA species in sperm most affected by paternal obesity, tRF5-GluCTC and miR-10, are heavily enriched in transcriptional regulatory functions, implying that changes in their abundance in sperm may perturb transcriptional regulation in the developing embryo post-transcriptionally. These targets are significantly downregulated by the 4-cell stage, when the MZT is complete; these early perturbations may set in train an altered physiology and reduced resilience to environmental insults (such as over-nutrition) in later life.

If the phenomenon we observe here translates to humans, our findings suggest that persons with obese paternal ancestry could avoid the deleterious effects of metabolic programming with dietary intervention, yet still propagate the propensity for metabolic dysfunction to their offspring. The implications for public health are obvious. Given that a wide range of phenotypes can be induced by a variety of paternal factors³⁷, it is not unreasonable to suppose that such epigenetic inheritance may propagate the risk of many human diseases. How the associated RNA perturbations induced by paternal obesity are maintained in germ cells and gametes an entire life cycle beyond the inducing stressor is currently a mystery.

Materials and methods

Mice and diets

All animals were handled in accordance with good practice as defined by the National Health and Medical Research Council (Australia) Statement on Animal Experimentation, and requirements of state government legislation. The study was approved by the Garvan/St Vincent's Animal Ethics Committee (12/09 and 13/35).

The A^{vy} mice used in this study were descended from an isogenic C57BL/6 colony at Oak Ridge National Laboratories (Oak Ridge, TN, USA), and have been maintained at the Victor Chang Cardiac Research Institute since 2001. A^{vy}/a mice display a variety of phenotypes from obese yellow through degrees of coat-colour mottling to lean agouti³⁸. To avoid any effects of ancestral obesity in our stock A^{vy} colony, we maintain it by breeding only lean agouti A^{vy}/a mice to congenic a/a mice. The breeding strategy is outlined in Supplementary Fig. 1, and breeding statistics in Supplementary Table 1. For experimental mice, yellow A^{vy}/a males were selected from the stock colony for mating to a/a females. For control mice, we paired a/a males and females from the stock colony and selected their offspring as founders, so that control founders were at least two generations removed from any heritable metabolic effects of the A^{vy} allele. Control mice were generated contemporaneously with PatOb mice over three generations, and pooled for analysis, after we ensured that metabolic characteristics of different generations of control mice were equivalent.

The mice in this study were produced over the course of two years in the same facility. To maximise breeding output (obese yellow A^{vy}/a mice are poor breeders), in general males were allowed to cohabit with females throughout the breeding period. To control for social effects on the females, some animals were time-mated: males were placed in the female's cage

overnight and removed early the next morning along with any faeces; this was repeated up to three times until a positive plug was observed.

All breeding mice were fed *ad libitum* on NIH-31 control diet from weaning (5% w/w fat, 13.5 MJ/kg). *a/a* experimental offspring were randomly assigned at weaning to either SF00-219 high-fat diet designed to mimic a Western fast-food diet (WD, equivalent to Harlan Teklad TD88137; 22% w/w fat (40% digestible energy), 19.4 MJ/kg, see Supplementary Table 2) or matched normal fat control (CD; 6% w/w fat, 16.1 MJ/kg, see Supplementary Table 2). Any $A^{vy/a}$ littermates in F1 were culled at weaning. Feeds were manufactured by Specialty Feeds (Glen Forrest, WA, Australia).

Experimental mice were culled at 12 weeks of age; metabolic organs were harvested and weighed and blood collected, and sperm were harvested from some animals (see below).

Metabolic profiling

Glucose tolerance testing was performed on six week old mice; the tester was unaware of the group allocation of the individuals being tested. Mice were fasted for 6 hours and given an intraperitoneal injection of 1.5 g glucose/kg weight. Blood glucose levels were measured at 0, 15, 30, 45, 60 and 90 minutes using an AlphaTrak glucose monitor (Abbott). Animals were excluded from the analysis if their blood glucose did not increase by at least 75% by 15 minutes post-injection, or if excessive fighting between animals before injection raised the basal glucose measurement more than two standard deviations above the group mean.

Serum insulin levels were measured in 12 week blood samples using the Mouse Insulin ELISA kit (Millipore); the tester was unaware of the group allocation of the samples being tested.

Lipidomic profiling was performed on 12 week liver samples, as described previously³⁹; the tester was blinded to the group allocation of samples. Samples more than two standard deviations from the group mean were excluded.

Sperm isolation and RNA preparation

Mature motile sperm were isolated from the cauda epididymis of 12 week old experimental mice on CD. Caudae were dissected and sliced open, and sperm allowed to swim out into DMEM media on a heating pad. Media was collected after 30 minutes and either snap frozen in liquid nitrogen or processed immediately. After thawing, samples were centrifuged at 50 g to remove any tissue debris. The supernatant was collected and sperm were centrifuged for 3 minutes at 2500 g, washed twice in PBS, incubated in somatic cell lysis buffer (0.5% Triton-X, 0.1% SDS) for five minutes, washed again and resuspended in PBS. A proportion of the sperm were examined microscopically for the presence of somatic cells: only sperm samples with no somatic cells visible in 500-1000 sperm visualised were used for RNA analysis. RNA was extracted from pelleted sperm using Trizol; sperm lysis was assisted by the addition of 200mM β -mercaptoethanol, and repeated passage through a 29g needle.

Small RNA-Seq

Barcoded small RNA sequencing libraries were prepared from ~100 ng sperm total RNA using the NEBNext Small RNA for Illumina kit (NEB). Ligation of the 3' adapter was allowed to proceed overnight to encourage maximal ligation of 3'O-methylated RNAs. Libraries were sequenced on an Illumina HiSeq 2500 in Rapid Run mode.

Fastq files were trimmed using Cutadapt (v1.6) to lengths of 18-51nt, with 10% adapter sequence error allowed. Trimmed reads were aligned to genome build mm10 using Bowtie (v1.1.1) with parameters: --sam -n 1 -l 18 -e 70 (one mismatch allowed in an 18 base seed

and a maximum sum of quality scores for mismatched bases of 70). Multimappers were randomly assigned among best hits. Mapped reads were annotated against miRNAs (mm10 mirbase20; mirbase.org), tRNAs (UCSC golden path), nested repeats (UCSC golden path), refgene (UCSC golden path) using custom perl scripts; annotation ties were broken by considering (in order) the orientation of the read relative to the genetic element, biotype hierarchy (according to the list above) and the number of bases overlapping the genetic element. For miRNA comparisons we used generalised linear modelling with EdgeR⁴⁰, applying an abundance threshold of 0.02% total miRNA (i.e. 200 reads per million mapped miRNA reads).

FLAG-Ago2 immunoprecipitation

HeLa cells were transfected with a FLAG-Ago2 construct in p3XFLAG-CMV-10 plasmid (Sigma). After 48 hours, $\sim 5 \times 10^6$ cells were lysed and the lysate incubated with Anti-Flag M2 antibody or isotype control IgG (Sigma) bound to Dynabeads Protein G (Life Technologies). After washing, 10% of the immunoprecipitation was removed for Western blotting for Flag-Ago2, and the remaining 90% was used for small RNA quantification. For RNA preparation, beads were treated with Proteinase K and removed, and RNA was prepared using Trizol.

tRF5-GluCTC, tRF5-GlyGCC and hsa-miR-21-5p were assayed in HeLa cell total RNA (to confirm tRF expression) and IP RNA (to test for Ago2 enrichment) by Taqman MicroRNA assay (Life Technologies).

miRNA/tRF target and GO analysis

To generate lists of target genes for miR-10a/b and tRF5-GluCTC, we used TargetScan v4.0, which allows input of a user-defined seed sequence⁴¹. We used DAVID^{42,43} to determine

significantly enriched ontologies. For analysis of miRNA/tRF target expression in oocytes and early embryo, we used data from DBTMEE²⁹ using an abundance threshold of 3 FKPM.

Statistical analyses

Weights trajectories were fitted using a linear mixed model⁴⁴ and comparisons performed with a Wald test. For metabolic measurements (GTT, serum insulin, liver lipids), groupwise comparisons were performed with one-way ANOVA. Because sample size was not equivalent between groups, we confirmed the homogeneity of variances using Levene's test. Where variances were unequal, Welch's modified F statistic was used to assess significance; equivalent conclusions were obtained using the Welch ANOVA and the standard ANOVA. Post-hoc pairwise comparisons between groups of interest were performed with a one-sided Student's t-test.

References

- 1 Hanson, M. A. & Gluckman, P. D. Early Developmental Conditioning of Later Health and Disease: Physiology or Pathophysiology? *Physiological Reviews* 94, 1027-1076, doi:10.1152/physrev.00029.2013 (2014).
- 2 Cropley, J. E., Dang, T. H., Martin, D. I. & Suter, C. M. The penetrance of an epigenetic trait in mice is progressively yet reversibly increased by selection and environment. *Proceedings of the Royal Society of London. Series B: Biological Sciences*, 2347-2353, doi:10.1098/rspb.2011.2646 (2012).
- 3 Sollars, V. *et al.* Evidence for an epigenetic mechanism by which Hsp90 acts as a capacitor for morphological evolution. *Nat Genet* 33, 70-74, doi:10.1038/ng1067ng1067 [pii] (2003).
- 4 Martinez, D. *et al.* In utero undernutrition in male mice programs liver lipid metabolism in the second-generation offspring involving altered Lxra DNA methylation. *Cell Metab* 19, 941-951, doi:10.1016/j.cmet.2014.03.026 (2014).
- 5 Jimenez-Chillaron, J. C. *et al.* Intergenerational transmission of glucose intolerance and obesity by in utero undernutrition in mice. *Diabetes* 58, 460-468 (2009).
- 6 Radford, E. J. *et al.* In utero undernourishment perturbs the adult sperm methylome and intergenerational metabolism. *Science*, doi:10.1126/science.1255903 (2014).
- 7 Aiken, C. E. & Ozanne, S. E. Transgenerational developmental programming. *Human Reproduction Update* 20, 63-75, doi:10.1093/humupd/dmt043 (2014).
- 8 Dias, B. G. & Ressler, K. J. Experimental evidence needed to demonstrate inter- and trans-generational effects of ancestral experiences in mammals. *Bioessays* 36, 919-923, doi:10.1002/bies.201400105 (2014).
- 9 Ng, S.-F. *et al.* Chronic high-fat diet in fathers programs β -cell dysfunction in female rat offspring. *Nature* 467, 963-969, doi:10.1038/nature09491 (2010).
- 10 Carone, B. R. *et al.* Paternally induced transgenerational environmental reprogramming of metabolic gene expression in mammals. *Cell* 143, 1084-1096, doi:S0092-8674(10)01426-1 [pii]10.1016/j.cell.2010.12.008 (2011).
- 11 Chen, Q. *et al.* Sperm tsRNAs contribute to intergenerational inheritance of an acquired metabolic disorder. *Science (New York, N.Y)* 351, 397-400, doi:10.1126/science.aad7977 (2016).
- 12 Pembrey, M. E. *et al.* Sex-specific, male-line transgenerational responses in humans. *Eur J Hum Genet* 14, 159-166, doi:5201538 [pii]10.1038/sj.ejhg.5201538 (2006).
- 13 Kaati, G., Bygren, L. O. & Edvinsson, S. Cardiovascular and diabetes mortality determined by nutrition during parents' and grandparents' slow growth period. *European Journal of Human Genetics* 10, 682-688, doi:10.1038/sj.ejhg.5200859 (2002).
- 14 Yen, T. T., Gill, A. M., Frigeri, L. G., Barsh, G. S. & Wolff, G. L. Obesity, diabetes, and neoplasia in yellow A(vy)/- mice: ectopic expression of the agouti gene. *FASEB J* 8, 479-488 (1994).
- 15 Zimmet, P., Alberti, K. G. & Shaw, J. Global and societal implications of the diabetes epidemic. *Nature* 414, 782-787, doi:10.1038/414782a (2001).
- 16 Perry, R. J., Samuel, V. T., Petersen, K. F. & Shulman, G. I. The role of hepatic lipids in hepatic insulin resistance and type 2 diabetes. *Nature* 510, 84-91, doi:10.1038/nature13478 (2014).
- 17 Moazed, D. Small RNAs in transcriptional gene silencing and genome defence. *Nature* 457, 413-420, doi:10.1038/nature07756 (2009).

- 18 Stuwe, E., Toth, K. F. & Aravin, A. A. Small but sturdy: small RNAs in cellular memory and epigenetics. *Genes and Development* 28, 423-431, doi:10.1101/gad.236414.113 (2014).
- 19 Ashe, A. *et al.* piRNAs can trigger a multigenerational epigenetic memory in the germline of *C. elegans*. *Cell* 150, 88-99, doi:10.1016/j.cell.2012.06.018 (2012).
- 20 Buckley, B. A. *et al.* A nuclear Argonaute promotes multigenerational epigenetic inheritance and germline immortality. *Nature* 489, 447-451, doi:10.1038/nature11352 (2012).
- 21 Rechavi, O. *et al.* Starvation-induced transgenerational inheritance of small RNAs in *C. elegans*. *Cell* 158, 277-287, doi:10.1016/j.cell.2014.06.020 (2014).
- 22 Grentzinger, T. *et al.* piRNA-mediated transgenerational inheritance of an acquired trait. *Genome Research*, doi:10.1101/gr.136614.111 (2012).
- 23 Sharma, U. *et al.* Biogenesis and function of tRNA fragments during sperm maturation and fertilization in mammals. *Science* 351, 391-396, doi:10.1126/science.aad6780 (2016).
- 24 Garcia-Silva, M. R., Cabrera-Cabrera, F., Guida, M. C. & Cayota, A. Hints of tRNA-Derived Small RNAs Role in RNA Silencing Mechanisms. *Genes (Basel)* 3, 603-614, doi:10.3390/genes3040603 (2012).
- 25 Kumar, P., Anaya, J., Mudunuri, S. B. & Dutta, A. Meta-analysis of tRNA derived RNA fragments reveals that they are evolutionarily conserved and associate with AGO proteins to recognize specific RNA targets. *BMC Biol* 12, 78, doi:10.1186/s12915-014-0078-0 (2014).
- 26 Sobala, A. & Hutvagner, G. Small RNAs derived from the 5' end of tRNA can inhibit protein translation in human cells. *RNA Biol* 10, 553-563, doi:10.4161/rna.24285 (2013).
- 27 Gebetsberger, J., Zywicki, M., Kunzi, A. & Polacek, N. tRNA-derived fragments target the ribosome and function as regulatory non-coding RNA in *Haloferax volcanii*. *Archaea* 2012, 260909, doi:10.1155/2012/260909 (2012).
- 28 Lykke-Andersen, K. *et al.* Maternal Argonaute 2 is essential for early mouse development at the maternal-zygotic transition. *Mol Biol Cell* 19, 4383-4392, doi:10.1091/mbc.E08-02-0219 (2008).
- 29 Park, S. J., Shirahige, K., Ohsugi, M. & Nakai, K. DBTMEE: a database of transcriptome in mouse early embryos. *Nucleic Acids Res*, doi:10.1093/nar/gku1001 (2014).
- 30 Dias, B. G. & Ressler, K. J. Parental olfactory experience influences behavior and neural structure in subsequent generations. *Nature Neuroscience* 17, 89-96, doi:10.1038/nn.3594nn.3594 [pii] (2014).
- 31 Alcazar, R. M., Lin, R. & Fire, A. Z. Transmission dynamics of heritable silencing induced by double-stranded RNA in *Caenorhabditis elegans*. *Genetics* 180, 1275-1288, doi:10.1534/genetics.108.089433 (2008).
- 32 Rassoulzadegan, M. *et al.* RNA-mediated non-mendelian inheritance of an epigenetic change in the mouse. *Nature* 441, 469-474, doi:10.1038/nature04674 (2006).
- 33 Wagner, K. D. *et al.* RNA induction and inheritance of epigenetic cardiac hypertrophy in the mouse. *Dev Cell* 14, 962-969, doi:10.1016/j.devcel.2008.03.009 (2008).
- 34 Gapp, K. *et al.* Implication of sperm RNAs in transgenerational inheritance of the effects of early trauma in mice. *Nat Neurosci* 17, 667-669, doi:10.1038/nn.3695 (2014).
- 35 Stoeckius, M., Grun, D. & Rajewsky, N. Paternal RNA contributions in the *Caenorhabditis elegans* zygote. *EMBO Journal* 33, 1740-1750, doi:10.15252/embj.201488117 (2014).

- 36 Stoeckius, M. *et al.* Global characterization of the oocyte-to-embryo transition in *Caenorhabditis elegans* uncovers a novel mRNA clearance mechanism. *EMBO Journal* 33, 1751-1766, doi:10.15252/embj.201488769 (2014).
- 37 Rando, O. J. Daddy issues: paternal effects on phenotype. *Cell* 151, 702-708, doi:10.1016/j.cell.2012.10.020 (2012).
- 38 Duhl, D. M., Vrieling, H., Miller, K. A., Wolff, G. L. & Barsh, G. S. Neomorphic agouti mutations in obese yellow mice. *Nat Genet* 8, 59-65, doi:10.1038/ng0994-59 (1994).
- 39 Matthews, V. B. *et al.* Interleukin-6-deficient mice develop hepatic inflammation and systemic insulin resistance. *Diabetologia* 53, 2431-2441, doi:10.1007/s00125-010-1865-y (2010).
- 40 Robinson, M. D., McCarthy, D. J. & Smyth, G. K. edgeR: a Bioconductor package for differential expression analysis of digital gene expression data. *Bioinformatics* 26, 139-140, doi:10.1093/bioinformatics/btp616 (2010).
- 41 Lewis, B. P., Burge, C. B. & Bartel, D. P. Conserved seed pairing, often flanked by adenosines, indicates that thousands of human genes are microRNA targets. *Cell* 120, 15-20, doi:10.1016/j.cell.2004.12.035 (2005).
- 42 Huang da, W., Sherman, B. T. & Lempicki, R. A. Systematic and integrative analysis of large gene lists using DAVID bioinformatics resources. *Nat Protoc* 4, 44-57, doi:10.1038/nprot.2008.211 (2009).
- 43 Huang da, W., Sherman, B. T. & Lempicki, R. A. Bioinformatics enrichment tools: paths toward the comprehensive functional analysis of large gene lists. *Nucleic Acids Res* 37, 1-13, doi:10.1093/nar/gkn923 (2009).
- 44 Laird, N. M. & Ware, J. H. Random-effects models for longitudinal data. *Biometrics* 38, 963-974 (1982).

Acknowledgements

Raw sequencing data has been deposited in the NCBI Sequencing Read Archive under study accession SRP051542. J.E.C. is supported by an Australian Research Council (ARC) DECRA Fellowship (DE120100723). G.H. is supported by an ARC Future Fellowship (FT110100455). M.A.F. is supported by an National Health and Medical Research Council (NHMRC) Senior Principal Research Fellowship (APP1021168). C.M.S. is supported by an ARC Future Fellowship (FT120100097). The study was supported by the Victor Chang Cardiac Research Institute, and in part by ARC DP120100825 and ARC DP130103027.

Author contributions

C.M.S. and J.E.C. conceived and designed the project with input from S.A.E. and D.I.K.M.; S.A.E. and A.A. performed animal husbandry and metabolic analyses, with assistance from P.E.Y., J.E.C. and M.E.B.; J.E.C. performed small RNA profiling; S.P.K. performed Ago2 immunoprecipitation and Taqman assays; P.E.Y., D.T.H, E.G. and J.W.K.H performed bioinformatics analysis; K.G.L. and D.C.H. performed mass spectrometry; C.M.S., J.E.C., M.F., G.H. and D.I.K.M. analysed and interpreted data; C.M.S., J.E.C. and D.I.K.M. wrote the paper, with input from all authors.

Competing financial interests

The authors declare no competing financial interests.

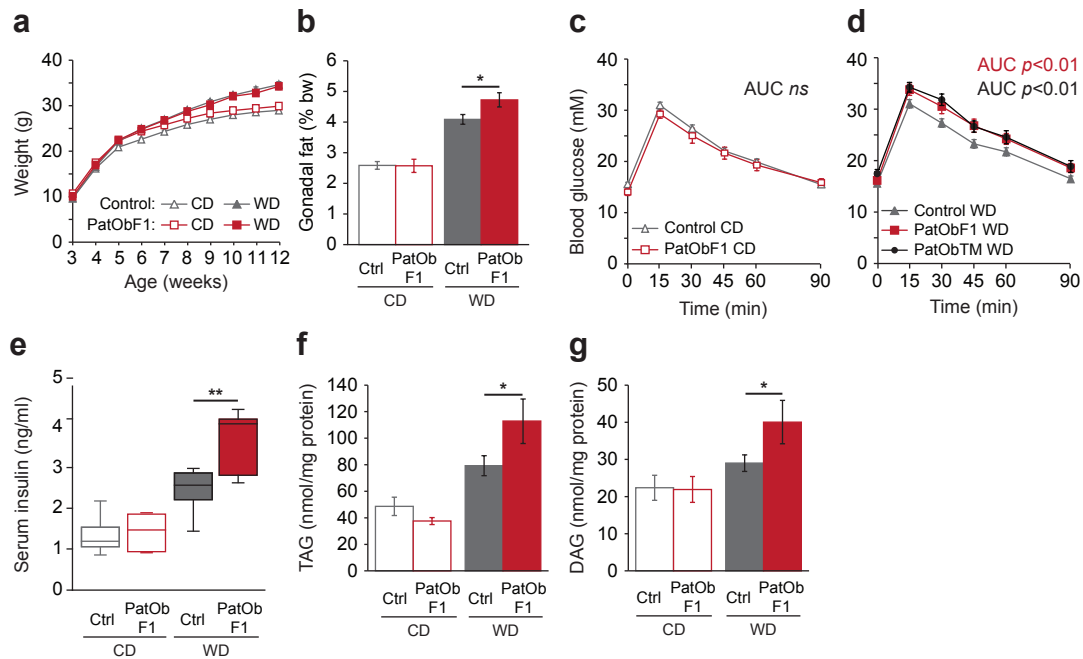


Fig. 1. Paternal obesity programs latent metabolic defects in F1 male offspring. (a, b) Body weights (a) and relative gonadal fat weights at 12 weeks (b) of Control and PatObF1 offspring fed control diet (CD) or Western diet (WD); CD: Control $n = 46$, PatOb $n = 16$; WD: Control $n = 43$, PatOb $n = 19$. (c, d) Glucose tolerance tests on six-week old CD offspring (c) and WD offspring (d), including those from time-mated obese sires (PatObTM, $n = 16$; other animal numbers as in a). (e) Serum insulin in 12-week old offspring; CD: Control $n = 9$, PatOb $n = 5$; WD: Control $n = 8$, PatOb $n = 5$. (f, g) Hepatic triacylglyceride (TAG, f) and diacylglyceride (DAG, g) levels in 12-week old offspring; CD: Control $n = 7$, PatOb $n = 8$; WD: Control $n = 8$, PatOb $n = 8$. Error bars represent SEM; * $p < 0.05$, ** $p < 0.01$.

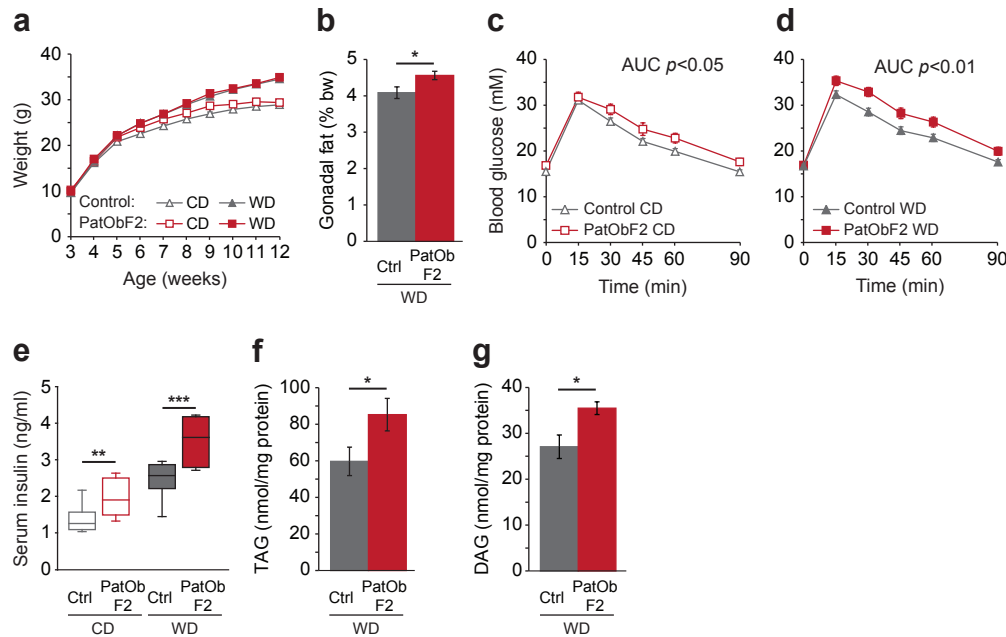


Fig. 2. Metabolic programming by paternal obesity is inherited by a second generation. (a) Body weights of Control and PatObF2 offspring fed control diet (CD) or Western diet (WD); CD: Control $n = 46$, PatObF2 $n = 17$; WD: Control $n = 43$, PatObF2 $n = 17$. (b) Relative gonadal fat weights in 12-week old mice; Control and PatObF2 animal numbers as in a. (c, d) Glucose tolerance tests on six week old CD (c) and WD (d) mice; animal numbers as in a. (e) Serum insulin in 12-week old mice; CD: Control $n = 9$, PatObF2 $n = 8$, WD: Control $n = 8$, PatObF2 $n = 7$. (f, g) Liver triacylglyceride (TAG, f) and diacylglyceride (DAG, g) levels in 12-week old mice on WD; Control, $n = 8$, PatObF2 $n = 7$. Error bars represent SEM; * $p < 0.05$, ** $p < 0.01$, *** $p < 0.001$.

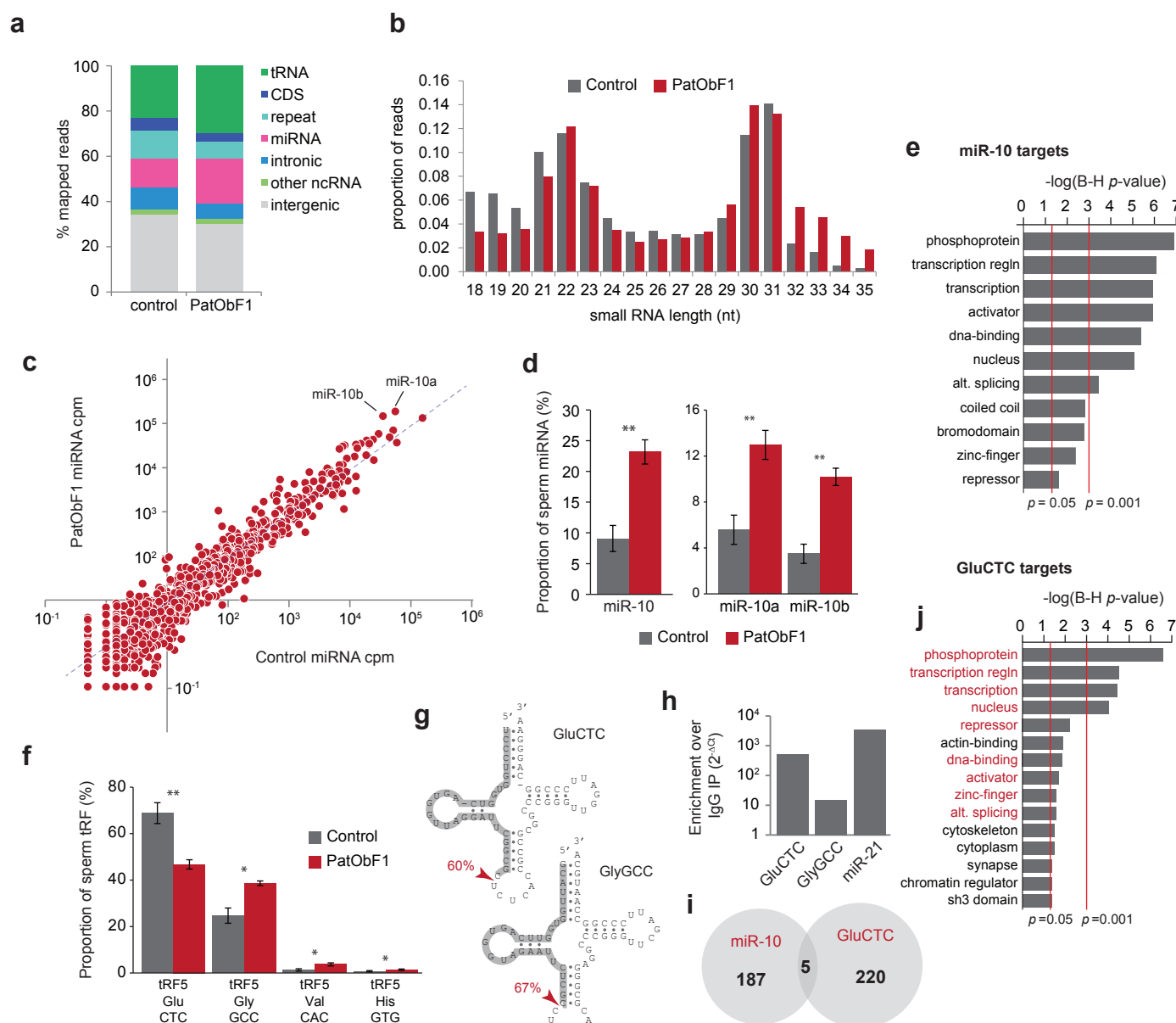
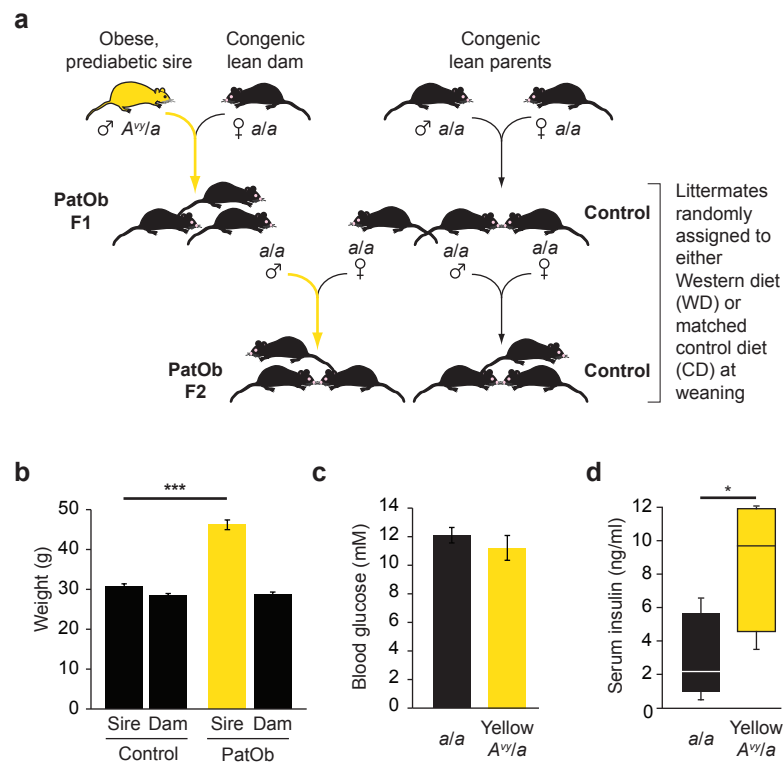
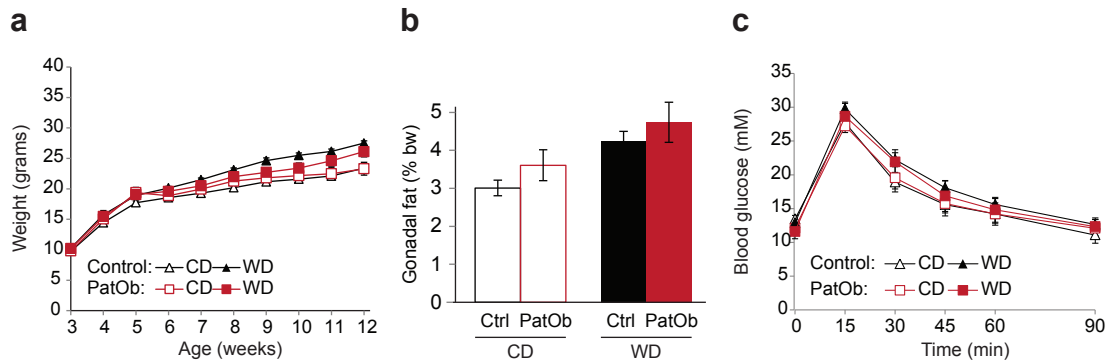


Fig. 3. Paternal obesity alters small RNAs in the sperm of F1 sons. Small RNA biotype (a) and size distribution (b) of all 18-35nt sRNA reads in Control and PatObF1 sperm. (c) Scatterplot of sperm miRNA abundance from Control (x-axis) versus PatObF1 (y-axis). (d) miR-10 as a fraction of all sperm miRNA in PatObF1 (red) relative to Control (grey); panel at right shows levels of the two miR-10 isoforms ** $q < 0.01$ (e) Gene ontologies significantly enriched in the targets of miR-10. (f) tRFs significantly altered in PatObF1 sperm (red) relative to control sperm (grey) represented as proportion of all sperm tRFs * $p < 0.05$, ** $p < 0.01$ (g) Clover leaf structures of GluCTC (top) and GlyGCC (bottom); dominant sperm tRF isoform shaded grey. (h) Results of Taqman RT-PCR on RNA purified from an Ago2 immunoprecipitation (IP) showing tRF enrichment in the IP over the negative control IgG IP; miR-21 is a positive control. (i) Individual gene targets of miR-10 and tRF5-Glu-CTC show little overlap. (j) Gene ontologies significantly enriched in the targets of tRF5-Glu-CTC; ontologies in common with miR-10 are shown in red.



Supplementary Figure 1. Experimental design and metabolic characteristics of obese founder males. (a) Schematic diagram showing breeding strategy. Obese yellow A^{vy}/a males were mated with congenic lean a/a dams to generate PatObF1. PatObF1 males were mated with Control F1 daughters, generated by mating lean a/a mice, to generate PatObF2. For simplicity, A^{vy}/a offspring of obese yellow A^{vy}/a sires are not shown. (b) Weights of lean a/a sires and their a/a dams (Control, $n = 62$) and of obese yellow A^{vy}/a sires and their a/a dams (PatOb, $n = 21$) measured one week after birth of offspring. (c) Blood glucose of lean a/a and obese yellow A^{vy}/a males at 12 weeks of age ($n = 12$). (d) Serum insulin of lean a/a and obese yellow A^{vy}/a males at 12 weeks of age ($n = 5$). Error bars represent SEM; * $p < 0.05$, *** $p < 0.001$.



Supplementary Figure 2. Female F1 offspring of obese sires are not fatter or predisposed to glucose intolerance. (a) Post-weaning weight trajectories of female offspring of obese sires (PatOb) or lean sires (Control), fed either Control diet (CD) or a Western diet (WD) (Control, $n = 19-20$; PatOb, $n = 7$). (b) Gonadal fat weight for female offspring as in a. (c) Glucose tolerance test at six weeks of age for F1 females, (Control, $n=16-19$; PatOb, $n = 7$).

Supplementary Table 1: Breeding statistics

Offspring Group	Sire genotype	Dam genotype	Number of sires	Number of litters	Average litter size ± SEM	Average sire age at birth ± SEM (d)	Average sire weight ± SEM (g) ^a
Control	<i>a/a</i>	<i>a/a</i>	15	23	6.8 ± 0.4	123 ± 9	31.1 ± 0.9
PatObF1	<i>A^{vy}/a</i>	<i>a/a</i>	8	12	7.4 ± 1.1	126 ± 11	48.6 ± 1.2***
PatObF2	<i>a/a</i>	<i>a/a</i>	6	15	6.9 ± 0.6	121 ± 12	33.5 ± 1.3

^a sire weight at 7dpp

*** $p < 0.0001$ v Control

Supplementary Table 2: Diets used in this study

	Western diet (SF00-219)	Control diet (SF04-057)
Protein	19.0%	19.0%
Total Fat	21.0%	6.0%
Crude Fibre	4.7%	4.7%
AD Fibre	4.7%	4.7%
Digestible Energy	19.4 MJ/Kg	16.1 MJ/Kg
% Total calculated digestible energy from lipids	40.0%	14.0%
% Total calculated digestible energy from protein	17.0%	21.0%
Ingredients		
Casein (Acid)	195 g/Kg	195 g/Kg
Sucrose	341 g/Kg	341 g/Kg
Canola Oil	nil	60 g/Kg
Clarified Butter (Ghee)	210 g/Kg	nil
Cellulose	50 g/Kg	50 g/Kg
Wheat Starch	154 g/Kg	306 g/Kg
DL Methionine	3.0 g/Kg	3.0 g/Kg
Calcium Carbonate	17.1 g/Kg	17.1 g/Kg
Sodium Chloride	2.6 g/Kg	2.6 g/Kg
AIN93 Trace Minerals	1.4 g/Kg	1.4 g/Kg
Potassium Citrate	2.6 g/Kg	2.5 g/Kg
Potassium Dihydrogen Phosphate	6.9 g/Kg	6.9 g/Kg
Potassium Sulphate	1.6 g/Kg	1.6 g/Kg
Choline Chloride (75%)	2.5 g/Kg	2.5 g/Kg
SF00-219 Vitamins	10 g/Kg	10 g/Kg
Cholesterol	1.5 g/Kg	1.5 g/Kg
Oxicap E2	0.04 g/Kg	0.04 g/Kg

Table S4: Genes targeted by tRF-GluCTC or miR-10 downregulated^a in the murine MZT

Entrez_ID	Gene	GluCTC target	mir-10 target	log ₂ (fold-change) 4C vs Oocyte ^b
13839	Epha5		Yes	-7.4
229011	Samd10	Yes		-5.3
12014	Bach2		Yes	-5.1
16591	Kl		Yes	-5.0
69727	Usp46		Yes	-5.0
244310	Dlgap2		Yes	-4.9
244654	Mtss1l		Yes	-4.5
239099	Homez		Yes	-4.5
27386	Npas3		Yes	-4.4
208439	Klhl29		Yes	-4.4
83922	Tsga14	Yes		-4.1
72333	Palld	Yes		-4.1
19013	Ppara		Yes	-4.0
11519	Add2	Yes		-4.0
64898	Lpin2	Yes		-4.0
58887	Repin1	Yes		-3.9
13358	Slc25a1		Yes	-3.9
319924	Apba1	Yes		-3.8
19684	Rdx	Yes		-3.8
22781	Ikzf4	Yes		-3.8
19883	Rora		Yes	-3.8
241656	Pak7	Yes		-3.7
13592	Ebf2		Yes	-3.7
11735	Ank3		Yes	-3.7
217335	Fbfl		Yes	-3.6
14768	Lanc11		Yes	-3.5
14007	Celf2		Yes	-3.5
72844	Kctd17		Yes	-3.5
11785	Apbb1	Yes		-3.4
22626	Slc23a3		Yes	-3.3
21388	Tbx5		Yes	-3.3
242481	Palm2		Yes	-3.3
217124	Ppp1r9b	Yes		-3.3
26381	Esrrg		Yes	-3.3
208869	Dock3	Yes		-3.2
432530	Adcy1	Yes		-3.1
109205	Sobp		Yes	-3.1

433926	Lrrc8b		Yes	-3.1
54338	Slc23a2	Yes		-3.1
14254	Flt1		Yes	-3.0
52588	Tspan14	Yes		-3.0
170826	Ppargc1b		Yes	-3.0
225743	Rnf165		Yes	-2.9
110279	Bcr		Yes	-2.9
99003	Qser1	Yes		-2.9
331474	Rgag4	Yes		-2.8
228790	Asx11	Yes		-2.8
15118	Has3		Yes	-2.8
18028	Nfib	Yes		-2.8
52428	Rhpn2		Yes	-2.7
71816	Rnf180		Yes	-2.7
54525	Syt7	Yes		-2.7
270201	Klhl18	Yes		-2.7
15571	Elavl3		Yes	-2.7
18645	Pfn2	Yes		-2.7
208151	Tmem132b		Yes	-2.6
214459	Fnbp11		Yes	-2.6
12325	Camk2g		Yes	-2.6
68737	Angel1	Yes		-2.6
76273	Ndfip2		Yes	-2.5
13544	Dvl3		Yes	-2.5
627214	Fam196a		Yes	-2.5
69274	Ctdspl		Yes	-2.4
15569	Elavl2		Yes	-2.4
234353	Psd3	Yes		-2.3
29867	Cabp1	Yes		-2.3
16594	Klc2		Yes	-2.3
19058	Ppp3r1	Yes		-2.2
75788	Smurf1		Yes	-2.2
94109	Csmd1		Yes	-2.2
20969	Sdc1		Yes	-2.2
213988	Tnrc6b		Yes	-2.1
116838	Rims2		Yes	-2.1
238988	Erc2	Yes		-2.0
74126	Syvn1	Yes		-2.0
12053	Bcl6		Yes	-2.0
17257	Mecp2	Yes		-2.0
338365	Slc41a2		Yes	-2.0

268980	Strn		Yes	-2.0
81489	Dnajb1	Yes		-1.9
14270	Srgap2	Yes		-1.8
12570	Cdk5r2	Yes		-1.8
18032	Nfix		Yes	-1.7
69288	Rhobtb1	Yes		-1.7
242443	Grin3a		Yes	-1.7
276952	Rasl10b	Yes		-1.6
75974	Dock11		Yes	-1.6
21844	Tiam1		Yes	-1.6
18569	Pdcd4	Yes		-1.5
231991	Creb5	Yes		-1.5
71865	Fbxo30		Yes	-1.5
330222	Sdk1		Yes	-1.5
76895	Bicd2		Yes	-1.3
320772	Mdga2		Yes	-1.3
17126	Smad2		Yes	-1.3
18141	Nup50		Yes	-1.3
269682	Golga3		Yes	-1.3
101488	Slco2b1	Yes		-1.2
12728	Cln5		Yes	-1.2
12125	Bcl2l11		Yes	-1.2
76686	Clip3	Yes		-1.2
23879	Fxr2	Yes	Yes	-1.2
217866	Cdc42bpb	Yes		-1.1
26403	Map3k11	Yes		-1.1
194655	Klf11		Yes	-1.1
20807	Srf	Yes		-1.1
212391	Lcor		Yes	-1.1
12703	Socs1	Yes		-1.1
26390	Mapkbp1		Yes	-1.0
12361	Cask		Yes	-1.0

^a $\log_2(\text{fold-change}) \leq -1$

^b Park, S. J., Shirahige, K., Ohsugi, M. & Nakai, K. DBTMEE: a database of transcriptome in mouse early embryos. Nucleic Acids Res (2014).

Table 1: microRNAs with altered abundance in sperm of PatObF1^a

	microRNA	Average counts per million ^b		Fold Change	q-value
		Control	PatOb		
Upregulated	mmu-miR-204	717	3,749	5.23	0.0002
	mmu-miR-182	694	2,298	3.31	0.0043
	mmu-miR-429-3p	386	1,182	3.06	0.0003
	mmu-miR-10b	35,008	101,932	2.91	0.0012
	mmu-miR-146b	566	1,634	2.88	0.0192
	mmu-miR-200a	280	793	2.83	0.0004
	mmu-miR-148a-3p	7,619	21,046	2.76	0.0033
	mmu-miR-200a-3p	6,752	18,443	2.73	0.0033
	mmu-miR-200b-3p	8,257	22,186	2.69	0.0039
	mmu-miR-451a	632	1,666	2.64	0.0257
	mmu-miR-183	1,226	2,985	2.44	0.0088
	mmu-miR-10a	55,867	129,719	2.32	0.0088
	mmu-let-7e	628	1,205	1.92	0.0267
	mmu-miR-210-3p	350	648	1.85	0.0266
	mmu-miR-187-3p	245	378	1.54	0.0438
Downregulated	mmu-miR-328-3p	1,661	582	0.35	0.0265
	mmu-miR-676-3p	2,003	699	0.35	0.0262
	mmu-miR-378a-3p	5,059	1,740	0.34	0.0246
	mmu-miR-669c	903	309	0.34	0.0433
	mmu-miR-92a-3p	12,593	4,390	0.35	0.0341
	mmu-miR-425	5,340	1,592	0.30	0.0405
	mmu-miR-127-3p	1,470	360	0.24	0.0033
	mmu-miR-184-3p	7,487	1,808	0.24	0.0103
	mmu-miR-34b-3p	12,678	2,073	0.16	0.0052

^a Where sequencing abundance > 200 reads per million and $q < 0.05$; ^b Reads per million mapped miRNA reads.